

Exploring the sources of p-mode frequency shifts in the CoRoT target HD 49933 *

Zhi-E Liu¹, Shao-Lan Bi¹, Wu-Ming Yang¹, Tan-Da Li², Kang Liu¹, Zhi-Jia Tian¹,
Zhi-Shuai Ge¹ and Jie Yu¹

¹ Department of Astronomy, Beijing Normal University, Beijing 100875, China;
zhiliu@mail.bnu.edu.cn

² Key Laboratory of Solar Activity, National Astronomical Observatories, Chinese Academy of
Science, Beijing 100012, China

Received 2013 November 25; accepted 2014 February 10

Abstract Oscillations of the solar-like star HD 49933 have been thoroughly observed by CoRoT. Two dozen frequency shifts, which are closely related to the change in magnetic activity, have been measured. To explore the effects of magnetic activity on frequency shifts, we calculate frequency shifts for the radial and $l = 1$ p-modes of HD 49933 with the general variational method, which evaluates the shifts using a spatial integral of the product of a kernel and some sources. The theoretical frequency shifts reproduce the observation well. The magnitudes and positions of the sources are determined according to a χ^2 criterion. We predict the source that contributes to both the $l = 0$ and $l = 1$ modes is located $0.48 - 0.62$ Mm below the surface of the star. In addition, based on the assumption that A_0 is proportional to the change in the MgII activity index Δi_{MgII} , we obtain that the change in MgII index between the minimum and maximum of the cycle during the period of HD 49933 is about 0.665. The magnitude of the frequency shifts compared to the Sun already demonstrates that HD 49933 is much more active than the Sun, which is further confirmed in this paper. Furthermore, our calculation of the frequency shifts for $l = 1$ modes indicates the variation of turbulent velocity in the stellar convective zone may be an important source for the $l = 1$ shifts.

Key words: stars: individual (HD 49933) — stars: evolution — stars: oscillation — stars: modeling

1 INTRODUCTION

HD 49933, also known as HR 2530 and HIP 32851, is an F5V main sequence star with a surface rotation period of 3.5 d. It has a temperature ranging between 6450 ± 75 K (Kallinger et al. 2010) and 6780 ± 130 K (Bruntt et al. 2004), a $\log(L/L_\odot)$ between 4.24 ± 0.13 (Bruntt et al. 2008) and 4.3 ± 0.2 (Bruntt et al. 2004) and a radius of $1.42 \pm 0.04 R(R_\odot)$. Its metallicity, ranging from -0.46 ± 0.08 (Bruntt et al. 2008) to -0.30 ± 0.11 (Bruntt et al. 2004), is slightly metal poor compared to the Sun and Procyon. All these characteristics are summarized in Table 1. Its oscillation, with

* Supported by the National Natural Science Foundation of China.

Table 1 Observational Data for HD 49933

T_{eff} (K)	$\log(L/L_{\odot})$	[Fe/H]	R (R_{\odot})	Reference
6570 ± 60		-0.44 ± 0.03		Bruntt (2009)
6450 ± 75				Kallinger et al. (2010)
6780 ± 130	4.24 ± 0.13	-0.46 ± 0.08		Bruntt et al. (2008)
6735 ± 53	4.26 ± 0.08	$-0.37 \pm 0.03^*$		Gillon & Magain (2006)
6780 ± 70	4.3 ± 0.2	-0.30 ± 0.11		Bruntt et al. (2004)
			$1.42 \pm 0.04^*$	Bigot et al. (2011)

* Data used by Liu et al. (2014).

Table 2 Observed Frequencies and Their Shifts for the Star HD 49933 (Salabert et al. 2011)*

Frequency (μHz) $l = 0$	Frequency shift (μHz)	Frequency (μHz) $l = 1$	Frequency shift (μHz)
1544.69 ± 0.83	0.753 ± 1.007	1500.54 ± 0.94	-0.336 ± 0.848
1631.10 ± 0.22	0.780 ± 1.123	1586.62 ± 0.61	-0.111 ± 0.666
1714.49 ± 0.61	-0.606 ± 2.108	1670.48 ± 0.81	1.139 ± 0.948
1799.75 ± 1.03	2.073 ± 1.508	1755.30 ± 0.78	-0.496 ± 0.981
1884.82 ± 0.59	0.815 ± 2.050	1840.68 ± 0.79	1.657 ± 0.853
1972.73 ± 1.14	1.344 ± 1.158	1928.13 ± 1.48	0.233 ± 0.750
2057.82 ± 0.96	3.059 ± 1.674	2014.38 ± 0.93	0.717 ± 0.992
2147.10 ± 1.05	2.808 ± 0.863	2101.58 ± 1.67	1.091 ± 1.021
2236.46 ± 0.39	1.868 ± 1.658	2190.81 ± 2.32	-0.578 ± 1.095
2322.10 ± 1.66	1.430 ± 2.193	2277.89 ± 1.29	-3.338 ± 1.826
2408.56 ± 0.83	2.174 ± 0.989	1500.54 ± 0.94	-0.336 ± 0.848
2495.76 ± 3.34	11.444 ± 2.812	1586.62 ± 0.61	-0.111 ± 0.666

* Data kindly provided through private communication.

the first observation of Doppler velocity done by Mosser et al. (2005), was observed three times by CoRoT in recent years, but the last run is still being processed by the CoRoT team. The time span of the first observation was 60 days at the beginning of 2007 during the first CoRoT run (IRa01) while the second was 137 days in 2008 during the first CoRoT long duration run (LRa01). García et al. (2010) analyzed these two sets of data and discovered that the p-mode frequencies and amplitudes of HD 49933 varied with magnetic activity and showed a period of at least 120 d. Subsequently, Salabert et al. (2011) analyzed the second set of data by dividing the 137-day light curve into two subseries corresponding to periods of low- and high-stellar activity based on the work of García et al. (2010). They extracted 24 frequencies and their shifts for $l = 0$ and $l = 1$ modes using a local maximum likelihood fitting analysis, which had 12 $l = 0$ modes and 12 $l = 1$ modes. These are listed in Table 2 (Salabert et al., private communication).

We can find from Table 2 that, for $l = 0$ modes, most frequency shifts are located in the range of 1–3 μHz , quite high compared to the frequency shifts of the Sun and β Hyi. In addition, the frequency shifts of HD 49933 reach a maximal value of about 3 μHz around 2100 μHz . For frequencies larger than 2100 μHz , the variation in the p-mode frequency shifts indicates a downturn followed by an upturn for both $l = 0$ and $l = 1$ modes. Such a frequency dependence of the frequency shifts measured in HD 49933 is comparable with the one observed in the Sun (Salabert et al. 2004), suggesting the solar-like star HD 49933 could have a similar physical mechanism driving the frequency shifts as the ones taking place in the Sun, which is thought to arise from changes in the outer layers due to its magnetic activity (Salabert et al. 2011).

In dynamo modeling, frequency shifts are thought to arise from either changes in propagation speed near the surface due to a direct magnetic perturbation (Goldreich et al. 1991), or a slight decrease in the radial component of the turbulent velocity in the outer layers and the associated

Table 3 Parameters for the Sun and β Hyi

Star	A_0	Ref.	Δi_{MgII}	Ref.	Frequency shift (μHz)	Ref.
Sun	0.3116	[1]	0.0135	[1]	most < 0.8	[1]
β Hyi	0.33	[1]	0.015	[1]	0.1 ± 0.4	[2]
HD 49933	14.63*		0.665*		most 1–3	[3]

[1] Metcalfe et al. (2007); [2] Bedding et al. (2007); [3] Salabert et al. (2011). *Results in this paper.

changes in temperature (Dziembowski & Goode 2004, 2005). Metcalfe et al. (2007) developed a method for predicting frequency shifts of solar-like stars based on scaling the measured p-mode frequency variations and changes in the chromospheric activity indices of the Sun. To forecast the frequency shifts, Metcalfe et al. (2007) resorted to the MgII index of the star and assumed that the relationship between variation of the MgII index and the source strength in the Sun is also valid in other stars. A specific forecast was made for the radial modes in the subgiant β Hyi, and results of their calculation were consistent with the observed shifts. This work was generalized to nonradial modes by Dziembowski (2007), with an additional assumption that the Sun and other stars share the same pattern in their butterfly diagrams.

In our previous work (Liu et al. 2014) we used the small frequency separation ratios r_{01} and r_{10} to constrain the evolution parameters of the stellar models and determined the size of the convective core and the extent of overshooting for HD 49933. In the present work, we will utilize the stellar models we have obtained in Liu et al. (2014), with the method developed by Metcalfe et al. (2007) to study the observed frequency shifts of HD 49933.

In Section 2 we outline the general variational method for modeling frequency shifts. Then we apply this method to study the shifts in radial and nonradial modes of HD 49933 in Section 3. Finally, we discuss our results and give conclusions in Section 4.

2 METHOD

2.1 General Formulations

In order to evaluate frequency shifts that are related to activity, we use a general variational expression given by Metcalfe et al. (2007),

$$\Delta\nu_{nlm} = \frac{\int d^3\mathbf{r} \mathcal{K}_{nlm} \mathcal{S}}{2I_{nl}\nu_{nlm}}, \quad (1)$$

where

$$I_{nl} = \int_0^R \rho \left[\xi_r^2 + \Lambda \xi_h^2 \right] r^2 dr = R^5 \bar{\rho} \tilde{I}_{nl} \quad (2)$$

is the mode inertia. $\Lambda = l(l+1)$ and $\bar{\rho}$ is the stellar mean density. The dimensionless mode inertia \tilde{I}_{nl} is defined as

$$\tilde{I}_{nl} = \int_0^1 \tilde{\rho} \left[y^2 + \Lambda z^2 \right] x^4 dx, \quad (3)$$

where $x = \frac{r}{R}$, $\tilde{\rho} = \frac{\rho}{\bar{\rho}}$, $y = \frac{\xi_r}{r}$ and $z = \frac{\xi_h}{r}$ are corresponding dimensionless quantities. Since all the derived kernels have leading terms proportional to $|\text{div } \boldsymbol{\xi}_{nlm}(\mathbf{r})|^2$, for simplicity Metcalfe et al. (2007) adopted the common kernel

$$\mathcal{K}_{nlm} = |\text{div } \boldsymbol{\xi}_{nlm}(\mathbf{r})|^2 = q_{nl}(D) |Y_l^m|^2, \quad (4)$$

where D denotes the depth below the photosphere and Y_l^m is the spherical harmonic. It is easily verified that

$$q_j(D) = \left[\frac{1}{r^2} \frac{\partial}{\partial r} (r^2 \xi_r(r)) - \frac{1}{r} \xi_h(r) \Lambda \right]^2. \quad (5)$$

The following simple form of the source was assumed in Metcalfe et al. (2007)

$$\mathcal{S}_k(D) = 1.5 \times 10^{-11} A_k \delta(D - D_{c,k}) \mu\text{Hz}^2, \quad (6)$$

where A_k and $D_{c,k}$ are adjustable parameters representing the strength and position of the source, respectively, and will be determined by fitting the measured shift data. The numerical factor is arbitrary. Combining Equations (6), (4) and (1) leads to

$$\Delta\nu_{nlm} = \frac{R}{M} \sum_{k=0}^l A_k Q_{nl}(D_{c,k}) \kappa_{k,lm}, \quad (7)$$

where

$$Q_{nl}(D_{c,k}) = 1.5 \times 10^{-11} \frac{q_j(D_{c,k})}{\tilde{I}_{nl} \nu_{nl}}, \quad (8)$$

$$\kappa_{nlm} = \int \int |Y_l^m|^2 P_{2k}(\mu) d\mu d\phi = \mathcal{P}_{2k}^l(m) Z_k^l \quad (9)$$

and

$$Z_{k,l} = (-1)^k \frac{(2k-1)!!(2l+1)!!(l-1)!}{k!(2l+2k+1)!!(l-k)!}. \quad (10)$$

In these equations, R and M are expressed in solar units, frequencies are expressed in μHz and $\mathcal{P}_{2k}^l(m) = lP_{2k}(m/l)$ are orthogonal polynomials of order $2k$ (see Schou et al. 1994).

2.2 Frequency Shifts of $l = 0$ and $l = 1$ Modes

Given the values of A_k and $D_{c,k}$, we can evaluate the change in the frequencies within individual multiples of low-degree modes using Equation (7). However, for radial modes ($l = 0$), both k and m only have single values that are zero, and thus only A_0 and $D_{c,0}$ are needed. Simple calculation shows $\kappa_{k,lm} = 1$ for $k = l = m = 0$. Then Equation (7) becomes

$$\Delta\nu_{n0} = \frac{R}{M} A_0 Q_{n0}(D_{c,0}). \quad (11)$$

The values of A_0 and $D_{c,0}$ can be determined by fitting the measured frequency shifts (see Table 2) for radial modes. Using the least squares fitting technique we have

$$A_0(D_{c,0}) = \frac{M \sum_n Q_{n0}(D_{c,0}) \Delta\nu_n^{\text{obs}} / (\sigma_{n0}^{\text{obs}})^2}{R \sum_n Q_{n0}^2(D_{c,0}) / (\sigma_{n0}^{\text{obs}})^2}, \quad (12)$$

where $\Delta\nu_{n0}^{\text{obs}}$ are the measured $l = 0$ shifts and σ_{n0}^{obs} are the measured uncertainties. For any given $D_{c,0}$, we can calculate A_0 through Equation (12) and $\Delta\nu_{n0}$ through Equation (11). By brute-force searching from the star's interior to the surface, we obtain the best estimate of $D_{c,0}$ that minimizes χ^2 (see Fig. 1)

$$\chi_0^2 = \sum_n \left(\frac{\Delta\nu_{n0} - \Delta\nu_{n0}^{\text{obs}}}{\sigma_{n0}^{\text{obs}}} \right)^2 = \sum_n \left[\frac{\frac{R}{M} A_0(D_{c,0}) Q_{n0}(D_{c,0}) - \Delta\nu_{n0}^{\text{obs}}}{\sigma_{n0}^{\text{obs}}} \right]^2. \quad (13)$$

It should be noted that Equations (12) and (13) are different from equations (8) and (9) in Metcalfe et al. (2007). The latter are problematic, because they always lead to too small A_0 and too large a discrepancy between calculated and measured shifts.

If we have measurements of the individual mode frequencies within multiplets, we could use Equation (7) to directly calculate A_k and $D_{c,k}$ for k up to l . However, such measurements are difficult, and we only get the mean frequency shifts (averaged over multiplet components) for $l = 1$ modes as shown in Table 2. In order to calculate the mean frequency shifts, the following formula is proposed in Dziembowski (2007)

$$\Delta\nu_{nl} = \frac{2l+1}{2} \frac{R}{M} \sum_{k=0}^l \left[\sum_{m=-l}^{m=l} |Y_l^m(\theta_0, 0)|^2 \kappa_{k,lm} \right] A_k Q_{nl}(D_{c,k}), \quad (14)$$

where θ_0 represents the inclination of the rotation axis to the line of sight. For $l = 1$ modes, there are two sources of perturbation that contribute to the frequency shifts, corresponding to $k = 0$ and $k = 1$ (see Eq. (6)), respectively. The above equation becomes

$$\begin{aligned} \Delta\nu_{n1} &= \frac{3}{2} \frac{R}{M} \sum_{k=0}^1 \left[\sum_{m=-1}^{m=1} |Y_1^m(\theta_0, 0)|^2 \kappa_{k,1m} \right] A_k Q_{n1}(D_{c,k}) \\ &= \frac{9}{8\pi} \frac{R}{M} A_0 Q_{n1}(D_{c,0}) + \frac{9}{40\pi} \frac{R}{M} (2 \cos^2 \theta_0 - \sin^2 \theta_0) A_1 Q_{n1}(D_{c,1}). \end{aligned} \quad (15)$$

Thus, four parameters, A_0 , A_1 , $D_{c,0}$ and $D_{c,1}$, in Equation (15) need to be determined. A_0 and $D_{c,0}$ can be determined through Equations (12) and (13), based on the frequency shift of radial modes, while A_1 and $D_{c,1}$ are calculated based on the frequency shift of $l = 1$ modes by minimizing the following χ^2 criterion

$$\chi_1^2 = \sum_n \left(\frac{\Delta\nu_{n1} - \Delta\nu_{n1}^{\text{obs}}}{\sigma_{n1}^{\text{obs}}} \right)^2, \quad (16)$$

with steps analogous to those used in calculating A_0 and $D_{c,0}$.

3 NUMERICAL RESULTS

3.1 Radial Modes

In order to calculate the frequency shifts of HD 49933 using Equation (11), a proper stellar model is needed. To reproduce the observed characteristics of HD 49933, in Liu et al. (2014) we computed a grid of evolutionary tracks with the Yale Rotation Evolution Code (Pinsonneault et al. 1989; Guenther et al. 1992; Yang & Bi 2007). The initial parameter range of masses and heavy metal abundances are $1.08 - 1.34 M_\odot$ and $0.006 - 0.030$, respectively. Theoretical analysis has been carried out for the star. A total of fifty-four best-fitting models were identified out of hundreds of evolutionary tracks in Liu et al. (2014), among which parameters of 17 models are listed in Table 4. These 17 models can not only reproduce, like the other 37 models, the measured temperature, luminosity, and large frequency separation of the star, but also fit the variation pattern of the small frequency separations well in terms of frequencies.

The computational results of all 17 models are summarized in Table 5. Here, we take model 16 from Table 4 as representative of our analysis, since it has the smallest χ_0^2 compared to other models. Among the 12 measured frequency shifts of radial modes, we rule out the last (and largest) shift and only fit the other 11 ones, because this shift is probably an outlier. Values of $\chi_0^2(r)$, defined by Equation (13), depend on the radius of the star. The variation of $\chi_0^2(r)$ with radius in the vicinity of the star's surface is shown in Figure 1. Note that in this figure, the χ_0^2 curve has two minima.

Table 4 Evolutionary Models (Liu et al. 2014) for HD 49933

Model	M (M_{\odot})	$(Z/X)_s$	T_{eff} (K)	L/L_{\odot}	R/R_{\odot} (R_{\odot})	Age (Gyr)
1	1.26	0.0061	6603	3.532	1.439	1.536
2	1.26	0.0073	6626	3.597	1.441	1.639
3	1.28	0.0097	6602	3.606	1.453	1.595
4	1.30	0.0092	6546	3.475	1.454	1.277
5	1.30	0.0106	6564	3.548	1.459	1.410
6	1.26	0.0059	6608	3.540	1.452	1.580
7	1.26	0.0071	6632	3.614	1.442	1.696
8	1.28	0.0069	6557	3.467	1.445	1.402
9	1.28	0.0082	6583	3.540	1.448	1.521
10	1.28	0.0094	6608	3.614	1.452	1.646
11	1.28	0.0135	6537	3.491	1.458	1.837
12	1.29	0.0132	6577	3.595	1.462	1.763
13	1.30	0.0104	6568	3.483	1.459	1.454
14	1.28	0.0133	6541	3.499	1.458	1.867
15	1.29	0.0125	6569	3.565	1.460	1.731
16	1.28	0.0131	6545	3.508	1.458	1.902
17	1.29	0.0123	6573	3.573	1.459	1.758

Table 5 Computational Results of the Evolutionary Models in Table 4

Model	A_0	$D_{c,0}$ (Mm)	Δi_{MgII}^*	χ_0^2	A_1	$D_{c,1}$ (Mm)	χ_1^2
1	13.57	0.527	0.617	2.734	-3814	3.842	7.675
2	12.93	0.516	0.588	2.699	-3749	3.806	7.764
3	14.23	0.561	0.647	2.700	-4149	3.868	7.810
4	15.16	0.554	0.689	2.748	-4421	3.910	7.685
5	16.55	0.620	0.752	2.735	-4720	3.985	7.749
6	13.49	0.528	0.613	2.742	-3737	3.818	7.658
7	13.20	0.534	0.600	2.702	-3689	3.801	7.719
8	14.46	0.539	0.657	2.761	-4084	3.872	7.638
9	14.14	0.543	0.643	2.723	-4105	3.874	7.719
10	14.18	0.564	0.645	2.707	-4069	3.857	7.787
11	12.76	0.484	0.580	2.644	-4133	3.745	7.933
12	14.23	0.557	0.647	2.643	-4288	3.825	7.898
13	15.14	0.577	0.688	2.736	-4369	3.897	7.745
14	13.49	0.513	0.613	2.641	-4179	3.758	7.921
15	12.91	0.504	0.587	2.672	-4085	3.785	7.870
16	14.63	0.558	0.665	2.639	-4333	3.809	7.886
17	13.69	0.534	0.622	2.672	-4221	3.832	7.869

* $\Delta i_{\text{MgII}} = A_0/22$.

However, the position of the source is unlikely to be determined by the left minimum, since the right one is a global minimum and the value of Q_{n0} at the left minimum is far lower than that at the right minimum. The best estimate of $D_{c,0}$, determined by the right minimum for χ_0^2 , is 0.558 Mm. The corresponding A_0 , obtained by Equation (12), is 14.63. The value of A_0 is much bigger than that of the Sun and β Hvi obtained by Metcalfe et al. (2007) (see Table 3). Considering that the measured frequency shifts for HD 49933 are quite large compared to those of the Sun and β Hvi, this result is not surprising. Because the value of A_0 is directly related to variation in the magnetic field near the convective zone of the star, we confirm that the magnetic field of HD 49933 shows more variations through the period of its cycle than the Sun or β Hvi.

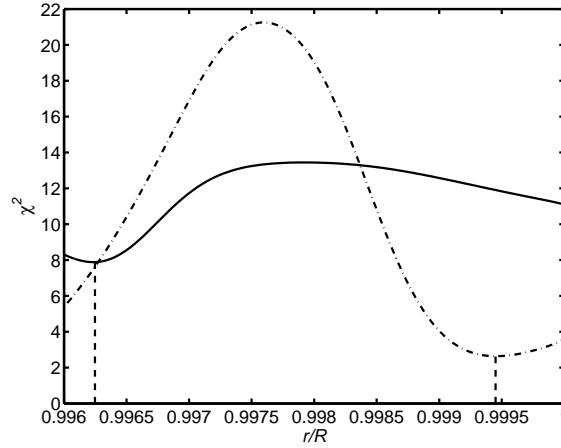


Fig. 1 χ_0^2 (dot-dashed line) and χ_1^2 (solid line) vs. relative radius r/R for model 16. The vertical lines mark the positions $D_{c,0}$ (right) and $D_{c,1}$ (left) of the source.

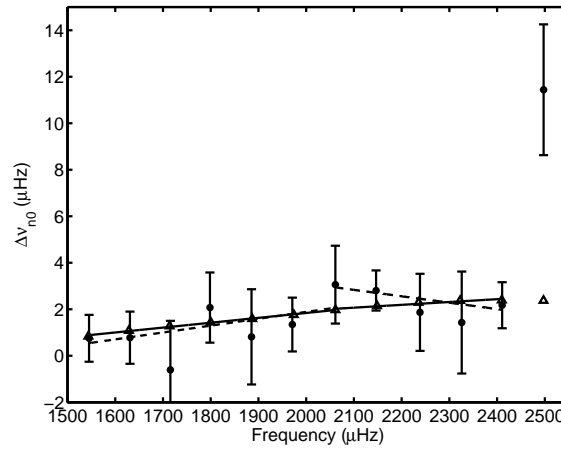


Fig. 2 Observed frequency shifts (dots) for the $l = 0$ mode of HD 49933 and theoretical results computed from Eq. (7) (triangles). The dashed lines correspond to weighted linear fits to the observed shifts, while the solid lines correspond to linear fits to the calculated shifts.

The frequency shifts calculated from Equation (11) for the radial modes of HD 49933, and the observed frequency shifts are shown in Figure 2. The corresponding least squares linear fits, for which the 1st to the 7th points and the 7th to the 11th points are fitted separately, are also drawn in the figure. A rising trend with increasing frequencies for the calculated shifts is evident, which is consistent with the results of previous work (Goldrich et al. 1991; Dziembowski & Goode 2004; Metcalfe et al. 2007). The measured shifts also grow with frequencies up to 2100 μHz (Salabert et al. 2011), but the four shifts in the range of 2100 – 2400 μHz seem to subsequently drop, which cannot be reproduced by the present model. However, due to the poor quality of observational data, this dropping pattern is questionable. Generally speaking, the calculations are in good agreement with the measurements. The value of χ_0^2 is 2.639.

The last measured frequency shift, whose value is $11.44 \mu\text{Hz}$, is exceedingly large compared to other measured frequency shifts. We cannot get a good fitting with it. Such a bimodal pattern, with different behaviors in low and high frequencies, was also found in frequency shifts of the Sun, for which the fractional frequency shifts rapidly rise at low frequencies and precipitously decline at high frequencies (above $\nu \approx 4 \text{ mHz}$). This behavior points to different locations of the sources producing the frequency shifts. Since Goldreich et al. (1991) ascribed the sudden decline in the solar frequency shifts at high frequencies to a rise in the solar chromospheric temperature, we naturally assume that it may be the decrease in the stellar chromospheric temperature that leads to the abrupt rise of frequency shift for HD 49933. The precipitous nature of the rise results from a chromospheric resonance that occurs at $\nu \approx 2500 \mu\text{Hz}$.

Unlike β Hyi and the Sun, which have been studied in Metcalfe et al. (2007), the measured MgII index data for HD 49933 are not currently available. Metcalfe et al. (2007) have obtained a relationship of $A_0 = 22\Delta i_{\text{MgII}}$ for the Sun. According to the assumption that the ratio between A_0 and Δi_{MgII} is invariant in different solar-like stars (Metcalfe et al. 2007), we can predict that the change in the MgII index between the minimum and maximum of the cycle during the period of HD 49933 should be about 0.665, a number yet to be validated by future observations.

3.2 Nonradial Modes

Benomar et al. (2009) measured the inclination angle of HD 49933 to be $\theta_0 = 17^\circ_{-9}^{+7}$. According to Equation (15), only A_1 depends on the value of θ_0 , but θ_0 has no impact on $D_{c,1}$ and the resulting χ_1^2 . So, we choose the central value of $\theta_0 = 17^\circ$ and calculate A_1 and $D_{c,1}$ by fitting the measured frequency shifts of $l = 1$ modes with the χ^2 criterion, i.e. Equation (16). In this calculation, we disregard the last observed frequency shifts.

The $\chi_1^2(r)$ curve in the vicinity of the star's surface is plotted in Figure 1. Figure 3 illustrates the calculated frequency shifts for the $l = 1$ modes, together with the observed data. We can see that though the agreement between theoretical results and measured shifts for $l = 1$ modes (with $\chi_1^2 = 7.886$) is not as good as that of the radial modes, the general trend of shifts with frequency is reproduced. The best estimate of $D_{c,1}$ is 3.809 Mm (see Fig. 1), which means the position of the

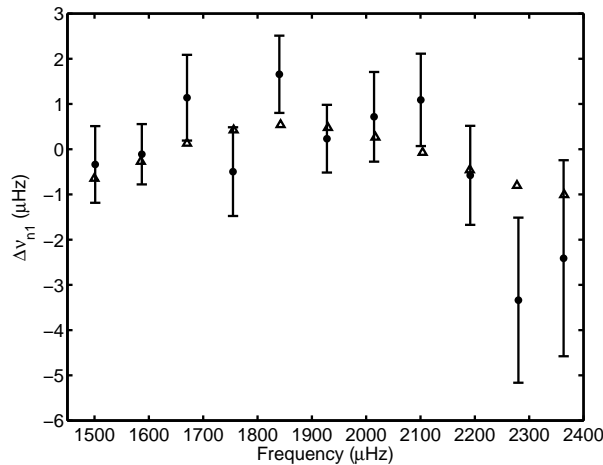


Fig. 3 The computed frequency shifts (*triangles*) and the measured shifts (*dots*) for $l = 1$ p-modes of HD 49933.

$k = 1$ source is deeper below the stellar surface than that of the $k = 0$ source. The calculated A_1 is negative, with a value of -4333 . This means the $k = 1$ source may represent a variation of turbulent velocity in the outer convective zone. It is commonly accepted that the magnetic field impedes convection, and so an increase in the magnetic field will reduce turbulent velocity. Dziembowski (2004) showed that a decrease in the turbulent pressure causes frequency to increase. Therefore, if we assume the variation of turbulent pressure in the stellar convective zone is a type of source, the corresponding A_1 should be negative.

4 DISCUSSION AND CONCLUSIONS

In this work, we reproduce the observed frequency shifts well for the radial ($l = 0$) and nonradial ($l = 1$) oscillation modes of a solar-like star HD 49933. Our results show that magnetic activity of HD 49933 may be more active than that of the Sun and β Hyi, and we predict the change in MgII activity index Δi_{MgII} between the minimum and maximum of the stellar activity cycle for HD 49933 should be much larger than that observed in the Sun and β Hyi. Moreover, the position of the source that contributes to both $l = 0$ and $l = 1$ modes is limited to be in the range $0.48 - 0.62$ Mm below the stellar surface.

It is commonly assumed that magnetic fields impede convection, that is, decrease the convective velocity. Our calculation for the frequency shifts of $l = 1$ modes indicates that the decrease in turbulent velocity induced by the increasing magnetic field in the rising phase during the active period of HD 49933 may significantly contribute to the frequency shifts for $l = 1$. Based on mixing-length theory, a decrease in the convective velocity is associated with a decrease in temperature in the convective zone (Dziembowski & Goode 2005), which can be reflected by lower effective temperature of a star. Since perturbations to effective temperature and chromospheric temperature are both related to activity in the magnetic field, the relationship between variations in the two types of temperatures during the cycle of stellar activity is also an issue deserving further research.

Acknowledgements We would like to thank D. Salabert for kindly providing us with the measured frequency shifts of HD 49933, and W. A. Dziembowski for his kind guidance in helping us to understand the method they developed. This work is supported by the National Natural Science Foundation of China (Grant Nos. 10933002, 11273007 and 11273012), and the Fundamental Research Funds for Central Universities.

References

- Bedding, T. R., Kjeldsen, H., Arentoft, T., et al. 2007, *ApJ*, 663, 1315
 Benomar, O., Baudin, F., Campante, T. L., et al. 2009, *A&A*, 507, L13
 Bigot, L., Mourard, D., Berio, P., et al. 2011, *A&A*, 534, L3
 Bruntt, H., 2009, *A&A*, 506, 235
 Bruntt, H., Bikmaev, I. F., Catala, C., et al. 2004, *A&A*, 425, 683
 Bruntt, H., De Cat, P., & Aerts, C. 2008, *A&A*, 478, 487
 Dziembowski, W. A., & Goode, P. R. 2004, *ApJ*, 600, 464
 Dziembowski, W. A., & Goode, P. R. 2005, *ApJ*, 625, 548
 Dziembowski, W. A. 2007, in *American Institute of Physics Conference Series*, 948, *Unsolved Problems in Stellar Physics: A Conference in Honor of Douglas Gough*, eds. R. J. Stancliffe, G. Houdek, R. G. Martin, & C. A. Tout, 287
 García, R. A., Mathur, S., Salabert, D., et al. 2010, *Science*, 329, 1032
 Gillon, M., & Magain, P. 2006, *A&A*, 448, 341
 Goldreich, P., Murray, N., Willette, G., & Kumar, P. 1991, *ApJ*, 370, 752

- Guenther, D. B., Demarque, P., Kim, Y.-C., & Pinsonneault, M. H. 1992, *ApJ*, 387, 372
- Kallinger, T., Gruberbauer, M., Guenther, D. B., Fossati, L., & Weiss, W. W. 2010, *A&A*, 510, A106
- Liu, Z., Yang, W., Bi, S., et al. 2014, *ApJ*, 780, 152
- Metcalfe, T. S., Dziembowski, W. A., Judge, P. G., & Snow, M. 2007, *MNRAS*, 379, L16
- Mosser, B., Bouchy, F., Catala, C., et al. 2005, *A&A*, 431, L13
- Pinsonneault, M. H., Kawaler, S. D., Sofia, S., & Demarque, P. 1989, *ApJ*, 338, 424
- Salabert, D., Fossat, E., Gelly, B., et al. 2004, *A&A*, 413, 1135
- Salabert, D., Régulo, C., Ballot, J., García, R. A., & Mathur, S. 2011, *A&A*, 530, A127
- Schou, J., Christensen-Dalsgaard, J., & Thompson, M. J. 1994, *ApJ*, 433, 389
- Yang, W. M., & Bi, S. L. 2007, *ApJ*, 658, L67